[19] Oftedahl, Chr., *Geol. Rundsch.*, **48**, 18 (1959).
[20] Heier, K. S., and Compston, W., *Lithos*, **2**, 133 (1969).
[21] Czamanske, G. K., *J. Geol.*, **73**, 293 (1965).
[22] Sceal, J. S. C., and Weaver, S. D., *Earth Planet. Sci. Lett.*, **12**, 327 (1971).
[23] Artemjev, M. E., and Artyushkov, E. V., *J. Geophys. Res.*, **76**, 1197 (1971).
[24] Khan, M. A., and Mansfield, J., *Nature Physical Science*, **229**, 72 (1971).
[25] Girdler, R. W., Fairhead, J. D., Searle, R. C., and Sowerbutts, W. T. C., *Nature*, **224**, 1178 (1969).
[26] Searle, R. C., *Geophys. J. Roy. Astron. Soc.*, **21**, 13 (1970).
[27] Griffiths, D. H., King, R. F., Khan, M. A., and Blundell, O. J., *Nature Physical Science*, **229**, 69 (1971).
[28] Talwani, M., Le Pichon, X., and Ewing, M., *J. Geophys. Res.*, **70**, 341 (1965).
[29] Freund, R., *Geol. Surv. Canada*, Paper 66-14, 471 (1964).
[30] Ramberg, H., *Lithos*, **4**, 259 (1971).
[31] Girdler, R. W., *Quart. J. Geol. Soc. London*, **114**, 79 (1958).
[32] Ansorge, J., Emter, D., Fuchs, K., Lauer, J. P., Mueller, St., and Peterschmitt, E., in *Graben Problems* (edit by Illies, J. H., and Mueller, St.), 190 (Schweizerbart, Stuttgart, 1970).
[33] Meissner, R., Berckhemer, H., Wilde, R., and Poursadeg, M., in *Graben Problems*, 184 (edit by Illies, J. H., and Mueller, St.), (Schweizerbart, Stuttgart, 1970).
[34] Pakiser, L. C., and Steinhart, J. S., *Res. Geophys.*, **2** (MIT, 1964).
[35] Thompson, G. A., and Talwani, M., *J. Geophys. Res.*, **69**, 4813 (1964).

New Deeps with Brines and Metalliferous Sediments in the Red Sea

H. BACKER & M. SCHOELL

Preussag, Hannover Bundesanstalt für Bodenforschung, Hannover

Investigation of Red Sea deeps has revealed 13 new brine pools and several areas covered by sediments of hydrothermal origin. There is a considerable variation of physical and chemical parameters within the sample of known Red Sea brines.

WATERS with anomalous salinity and temperature associated with metalliferous sediments have been known since 1964 near the central rift zone of the Red Sea between Djidda and Abu Shagara.

Following discoveries made from the Swedish vessel Albatross in 1948 (ref. 1), the brine area was intensively investigated from 1964 to 1966 (refs. 2–5). The result was the discovery and detailed description of three brine pools, the most important one being Atlantis II Deep[3]. Outside the Atlantis II Deep area only one indication (echo reflexions) has been reported from a deep near Brother Islands[5]. Tooms (personal communication) confirmed the existence of brines in that area and found sediments of hydrothermal origin in the Nereus Deep. These and additional observations called for a general survey of the whole central Red Sea trough. A general distribution of brine activity should have principal implications on the genesis of this type of ore deposit.

The whole central rift from Subair Islands to Abulkizaan (Daedalus Reef) has now been mapped using land-bound navigation systems (Shoran and Decca hi-fix) and a stabilized narrow-beam echo sounder (ELAC Schelfrandlot, 30 kc, beam width ±1.4°). For comparison, the Gulf of Aden rift system was included. During two Valdivia cruises, 13 new brine pools and several areas covered by sediments of hydrothermal origin were found. Compared with the well-known Atlantis II Deep area some of these findings show a remarkable variety of physical parameters and chemical components.

Some Aspects of the General Geological Setting

The bathymetric survey of the Red Sea rift system revealed considerable differences in the tectonic patterns between the southern and the central part of the Red Sea. In the area from Nereus Deep to the Suakin Deep the sea floor on both sides precipitates directly from the reefs down to a depth of 500–600 m, from where the bottom slopes only slightly over a distance of about 40 km to the edge of the main trough (at about 1,100 m), from which it reaches the final depth after a steep slope. Locally the central trough is flanked by high tectonic escarpments. In some cases there are two or three parallel basins with small ridges in between (Suakin Deep, Port Sudan/Volcano Deeps, Nereus Deep). In the Atlantis II Deep area five such parallel basins can be distinguished.

The rift system in the southern Red Sea from Suakin Deep to Djebel Tair is characterized by typical graben–horst structures. Long, flat-bottomed terraces and deeps are

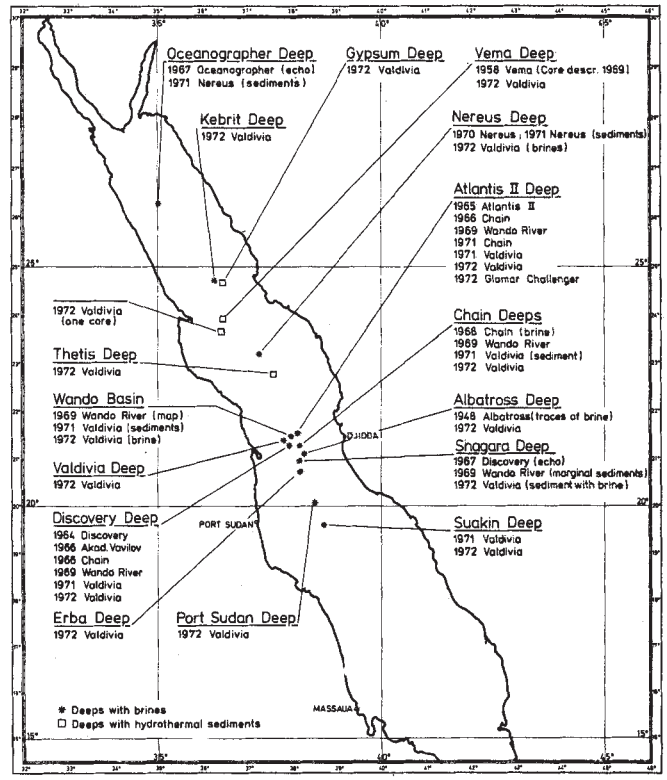

Fig. 1 Distribution of brine pools and brine derived sediments in the Red Sea. Principal investigations until May 1972.

accompanied by high ridges which are often delimited by steep scarps. Contrary to the northern Red Sea there is a central rough zone (similar to the Gulf of Aden) forming the deepest part of the sea. But the accompanying graben structures on both sides are only a few hundred metres higher.

This morphological situation is not very favourable for a transport of formation waters from the marginal evaporite bearing zones to the active central rough zone which offers the only significant trap structures with suitable low pelagic sedimentation rates. The different tectonic situation described is reflected by the geographic distribution of the brine pools discovered.

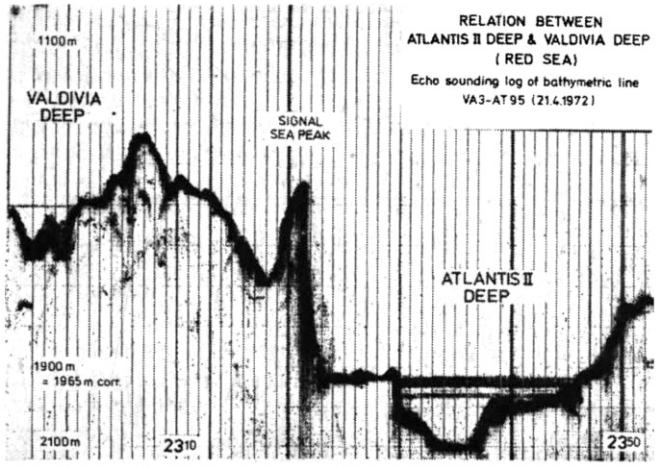

Fig. 2 Original echo sounding log of a profile in the Red Sea rift valley from Valdivia Deep (23.00: 21° 20.3′ N; 37° 56.9′ E) to Atlantis II Deep (23.50: 21° 21.2′ N; 38° 08.0′ E). ELAC narrow beam echo sounder 30 kc ±1.4° beam width. Direction of the section 86°. The horizontal echoes correspond to the surface of brine layers.

A further new aspect of the general geologic situation in the Red Sea rift system is the proof of an extensive volcanic activity throughout the whole area. During our investigations 53 samples of tholeiitic basalts and basaltic glasses were collected along the main trough of the Red Sea between Hanish Islands and 23° N.

Besides the known volcanic surface structures of the central rift (Hanish and Subair Island, Djebel Tair and Suburged) a submarine volcano ("Ramad Seamount") has been found at 17° 00′ N and 40° 40′ E. Its flanks are covered with black ashes. Similar pyroclastites were found in a deep ("Volcano Deep" near Port Sudan Deep) at a depth of 2,440 m at 20° 01.3′ N and 38° 27.0′ E. Evidence of volcanic activity in the Atlantis II Deep is given by several lava flows which are intercalated in the hydrothermal sediments.

Tectonic and volcanic activity is reflected by the recently observed earthquake intensities. Epicentres have been registered during the past few years mainly in the Gulf of Aden and the southern Red Sea[6]. Two important groups are situated around Port Sudan Deep and Suakin Deep. The detailed analysis of one earthquake (March 31, 1969) in the northern Red Sea revealed the extent of important dislocations[7].

Many new heat flow measurements in the Red Sea and Gulf of Aden show in general high values and are in agreement with previously published data[8]. They range within values typical of mid-ocean ridges. Extreme values are connected with Atlantis II Deep, Suakin Deep and Nereus Deep, where they are found in marginal zones (J. Scheuch and R. Hänel, personal communication).

Evaporites seem to be one prerequisite for the formation of the Red Sea brines[5]. Miocene evaporites including large quantities of rock salt are described from wells and outcrops along the Red Sea from the Gulf of Suez to the Dakhlak Islands and even near Atlantis II Deep (R. D. Whitmarsh, personal communication). This sequence probably underlies large areas of the Red Sea basin and is covered by only a few hundred metres of Plio-Pleistocene calcareous clays and microfossiliferous oozes. Thus the evaporites can easily come into contact with the seawater during tectonic displacements near the surface.

The place of the different brine pools within the described geological setting is chiefly governed by recent tectonic lines. The brine basins generally occupy the deepest parts of local basins within the main central rift and are delimited by NW-striking faults. There are a few significant exceptions: Valdivia Deep (1,673 m) is a special depression on the slope of the central trough (2,200 m). Further, some of the deeps

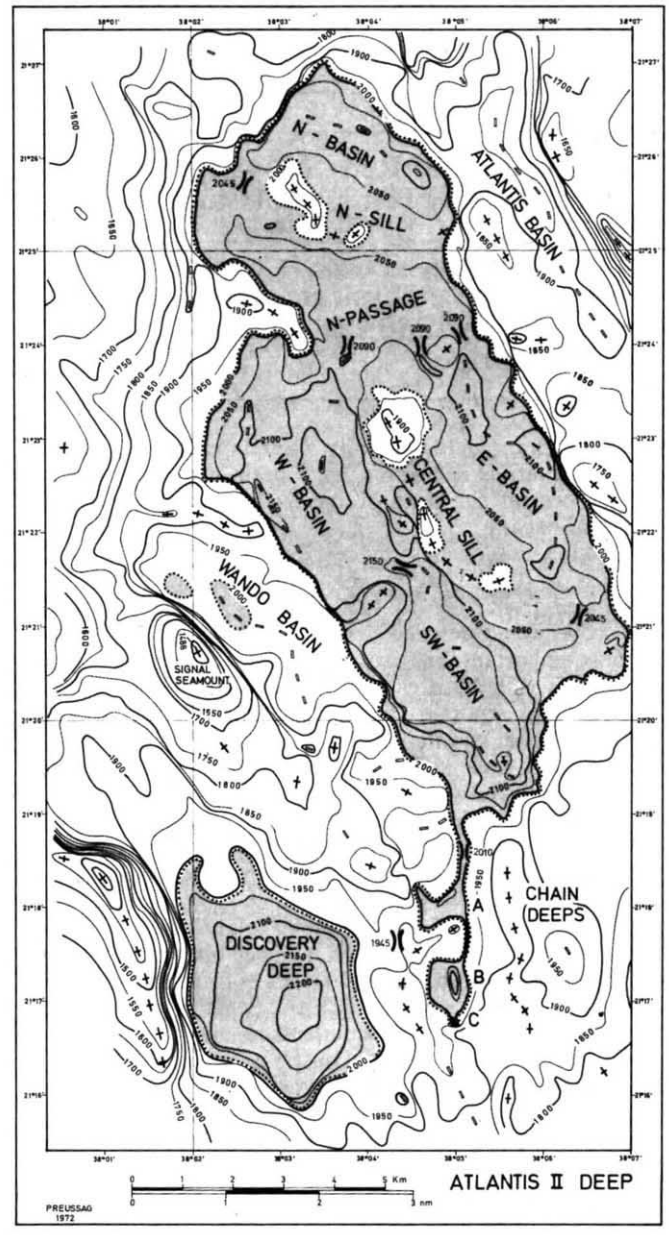

Fig. 3 Bathymetric chart of the Atlantis II Deep area, Red Sea. ELAC narrow beam echo sounder (30 kHz ±1.4° beam width). Contours in metre, corrected after Matthews[13]. Decca hi-fix navigation. Track space 400 m, within the Atlantis II Deep and Chain Deeps 100 m. Dotted line uppermost echo reflector on top brine.

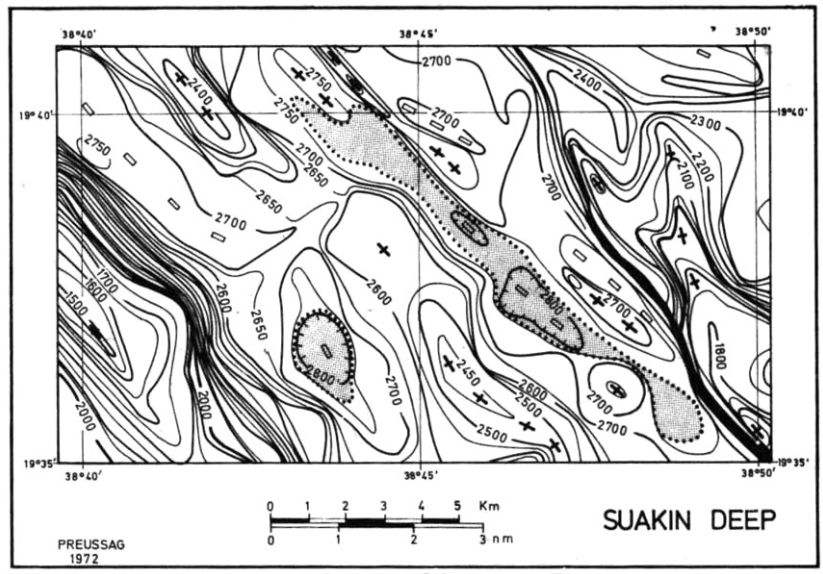

Fig. 4 Bathymetric chart of the central part of the Suakin Deep. Explanation see Fig. 3. Track space 1.4 km, locally less.

(Valdivia, Kebrit and Discovery Deep) are more or less round structures not consistent with the general tectonic trends. The Albatross Deep has a unique position: any rise of the present brine level would cause an overflow into the Shagara Deep, the bottom of which is roughly 400 m below the Albatross Deep.

The Brines

Generally the deeps are filled with brines of different salt concentrations, the most concentrated one forming the principal and the lowermost brine layer. The development of the transition zone (that is, the mixing zone to the overlying seawater) is different. For some deeps a layered transition zone is characteristic (stepwise increase of temperature and chlorinity).

The most characteristic examples in this case are the Atlantis II Deep and nearby deeps. Similar stratifications have been detected in the Suakin Deep and the Port Sudan Deep. For all other deeps small undifferentiated transition zones are typical.

At least one of the brine pools now known is in an active state (Atlantis II Deep). Many observations since 1964 revealed a continuous rise of temperatures (1965–1972, 55.9° C–60.1° C). Convection currents are indicated by direct measurements (D. L. Dorson, personal communication) and have been confirmed by detailed temperature profiles[11]. As a consequence of this the 59–60° C brine which originates in the Atlantis II Deep SW basin is at the moment spreading to the other basins of the brine pool[11].

For the chemical characterization of the brines, their content in Cl, SO_4, Ca, Mg, Fe, Mn, Zn, Cu and the gases H_2S and CO_2 is most important. The Atlantis II Deep and neighbouring depressions have the highest chlorinities. In some areas with abundant hydrothermal sediments, however, only a very slight increase of the chlorinities could be detected in the connate water (Thetis, Vema and Gypsum Deeps). The Mg and SO_4 depletion observed in the Atlantis II Deep brine by several authors could not be found in the other deeps except those near the Atlantis II Deep and (for SO_4) in the Nereus Deep. Carbon dioxide was found in the Valdivia and Kebrit Deeps and in the Atlantis II Deep[9] in various concentrations. Hydrogen sulphide is present in remarkable quantities in the Kebrit Deep and gives rise to its name. The presence of H_2S in the incoming brine of Atlantis II Deep must also be concluded from the high amount of monosulphides in the recent sediments.

Some adacent brine pools without "surface" connexions do not seem to be entirely separated. Evident conformity of the physical parameters and the chemical composition were detected suggesting subsurface connexions in the case of three groups of deeps: Atlantis II Deep with Discovery and Chain Deeps as well as Wando Basin; the two brine pools in Suakin Deep; the two basins of Nereus Deep.

The Sediments

Normal sediments in the central trough of the Red Sea are light-coloured marls with, in most cases, a significant content of nannofossils and pelagic microfossils, especially globigerinids and pteropods. Brownish coloured layers with

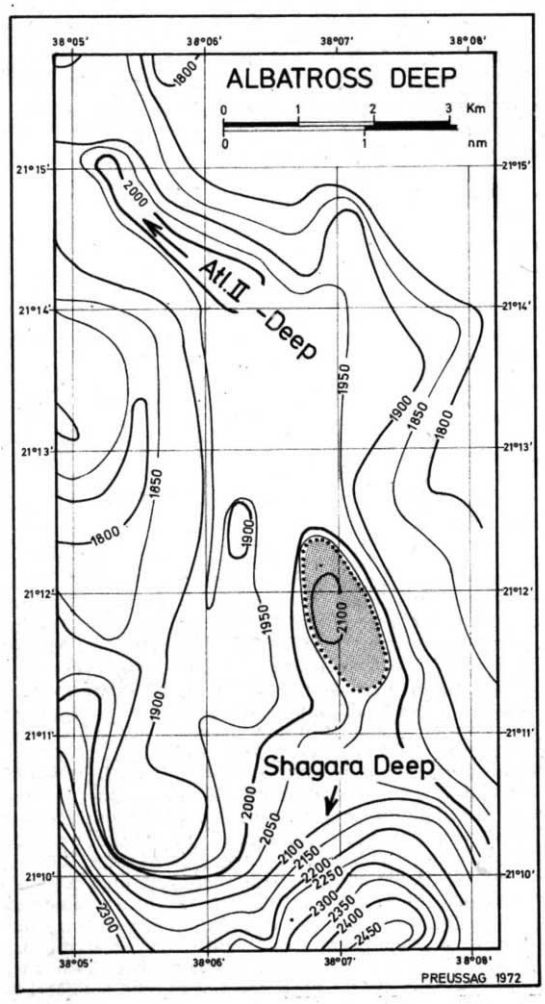

Fig. 5 Bathymetric chart of the Albatross Deep area. Explanation see Fig. 3. Track space about 1 km.

Table 1 Brine Filled Basins and Major Indications of Hydrothermal Sediments in the Red Sea Rift Zone

Name	Geographic coordinates of the centre of the brine covered areas or of the whole deep if no brine is present N	E	free brine surface	important hydroth. sediment	Total depth	Top brine (uppermost echo reflector)	Max. thickness of brine layer	brine surface (approximative, km²)	number of echo reflectors (thickness of reflector system)	sound velocity in the main brine (m/s)	saltcontent of most concentrated brine (chlorinity, ‰ Cl,)	Temperature of brine °C max.	rising downward	± constant	decreasing downward	some variable brine components Mg	Ca	Zn·10⁻³	SO₄ g/kg	main dissolved gases N_2	CO_2	H_2S	CH_4	C_2H_6
Suakin Deep SW Basin	19° 36,7'	38° 43,6'	+	+	2850	2776	74	2,5	1	1703	85,8	23,9	+			1,4	2,1	0,05	3,2					
Suakin Deep NE Basin	19° 38,0'	38° 46,3'	+	+	2830	2776 (2743)	54 (87)	10	1 3	1704	85,9	24,6	+			1,4	2,2	0,04	3,2					
Port Sudan Deep	20° 3,8'	38° 30,8'	+	+	2800 2836	2514	286 322	5	3 (15m)	1795	125	36,2	+			1,5	1,1	0,17	4,0					
Erba Deep	20° 43,8'	38° 11,0'	+	(+)	2395	2376	19	7	2-3 (15m)		86,5 (2386m)	27,9 (2389m)	+			1,5	1,0	0,36	4,1					
Shagara Deep	21° 7,8'	38° 5,3'	+	+	2496	2488	8	1	1		113													
Albatross Deep	21° 11,9'	38° 7,0'	+	+	2133	2051	72	1,5	1	1797	143,3	24,4			+									
Chain Deep C	21° 16,77'	38° 4,95'	+		2165?	1998?	167?	0,02		1820	154,6	44,5	+											
Chain Deep B	21° 17,17'	38° 4,95'	+	+	2130	1990	140	0,8	1 (2?)	1825	156,0	46,3 46,7	+	+										
Chain Deep A (North)	21° 18,0'	38° 4,9'	+	+	2072	1989 (2005)	83 (67)	0,7	5	1821	153,8 (2052m)	52,1 53,2	+		+									
Discovery Deep	21° 17,0'	38° 3,2'	+	+	2224	2015 2049	209 175	11,5	5-7 (34m)	1824	155,5	44,8	+	+	+	0,8	5,1	0,8	0,6					
Wando Basin	W: 21° 21,45' E: 21° 21,20'	38° 1,80' 38° 2,40'	+	+ +	2013 2007	1985 1985	28 22	0,2 0,5	1-2 2	1673	73,5	24,1 29,3	+											
Atlantis II Deep	21° 22,5'	38° 4,5'	+	+ +	2170 2194	1992	178 126	55	7-10 (52m)	1821 1830	156,5	60,0 60,1	+	+		0,7	5,2	5,4	0,8	+	+		+	+
Valdivia Deep	21° 20,5'	37° 57,0'	+	–	1673	1550	123	4	1	1806	136,6 144,7	29,5 29,8	+			1,9	0,8	0,4	6,8	+	+		+	tr
Thetis Deep	22° 43'	37° 36'	–	+ +	1970 1819						22,9	22,6			+									
Nereus Deep E Basin	23° 11,5'	37° 15'	+	+	2458	2419	39	3	1	1675	129,5	30,2	+		+	1,5	7,9	0,5	0,9	+	tr		tr	
Nereus Deep W Basin	23° 11'	37° 12'	+	+	2432	2421	11	1	1															
Vema Deep	23° 52,0'	36° 30,5'	–	+	1611						22,7													
Gypsum Deep	24° 42,1'	36° 24,8'	–	+ +	1196						23,7													
Kebrit Deep	24° 43,35'	36° 16,6'	+	–	1558 1573	1466	92 107	2,5	1	1810	153,3	23,3		+		2,4	1,7		2,2	+	+ +	+ +	+	+
Oceanographer Deep	26° 17,2'	35° 1,0'	+	–	>1446	~1364	>82		1															
Normal Red Sea water					2850					1570	22,5	21,8		+		1,41	0,45		2,96					

1, Bathysonde; 2, reversal thermometers; 3, both reversal thermometers and bathysonde; 4, ref. 5; 5, uncertain; 6, corrected approximately with sound velocity in the brine; 7, calculated from distances of echoes of water samplers on the echosounder log, approximately[12]; 8, in the area now covered by brine little sediment; 9, the whole Shagara Deep is 12 km in diameter; 10, probably identical with that described in the Discovery account[5]; 11, meter, corrected after Matthews; 12, connate water; 13, information from ref. 5 and Tooms (personal communication); 14, lowermost part; 15, 1971; 16, 1972; 17, 1971 and 1972; 18, identical with that described by Ross and Hunt[4]; 19, two groups; 20, top of the second package of reflecting layers; water above without significantly higher salinity; 21, connexion by a channel with Atlantis II Deep; 22, top of the lowermost reflector, corresponding approximately to the top of the main brine layer; 23, main brine layer; 24, two small areas are now covered with brine which are possibly connected; 25, mainly data from the SW Basin 1972; 26, locally not very distinct reflecting layers are visible up to 1,971 m corrected; the top of the lowermost reflector, corresponding with the top of the 60° C brine is at 2,044 m (after Matthews[13], probably 2,049 m with consideration of higher velocity in the brine); 27, only the undiluted 60° C brine; thickness with consideration of sound velocity in brine about 150 m; 28, the brine pool has a length of 14 km and a maximum width of 1.5 km; 29, Suakin Deep SW Basin is probably the deepest point of the Red Sea; "corrected" depth values range up to 2,867 m, but the cable length was slightly less; 30, locally; 31, including a small brine pool NW from the main trough which might be separated by a low sill; the brine reflector appears about 2 m deeper; 32, around 2,000 m; 33, ref. 5: sea-water with 21.13 g kg^{-1} Cl; 34, the Gypsum Deep area is only a shallow depression but contains sediments with high content of hydrothermal material; 35, though there seems to be no free brine surface, a slightly elevated salinity was found in water from a piston core liner; 36, Thetis Deep, named after the nearby Thetis Reef, has a surface of about 20 by 30 km and consists of several more or less separated individual basins; the most important hydrothermal influences within the Thetis Deep are in the North Basin with a surface of approximately 3 by 10 km; 37, North-Basin; 38, at 1,800 m in the N-Basin; 39, Vema Deep measures about 24 by 6 km; sediments with hydrothermal components were first sampled by R/V Vema, ref. 5; 40, shipboard Mohr-Knudsen titrations; 41, the uppermost echo reflector corresponds generally with the first significant salinity increase[11]; 42, differentiated, for details see ref. 11; 43, in the main brine, two layers can be distinguished; the lower one (about 40 m) has a slightly higher temperature and a significantly higher chlorinity.

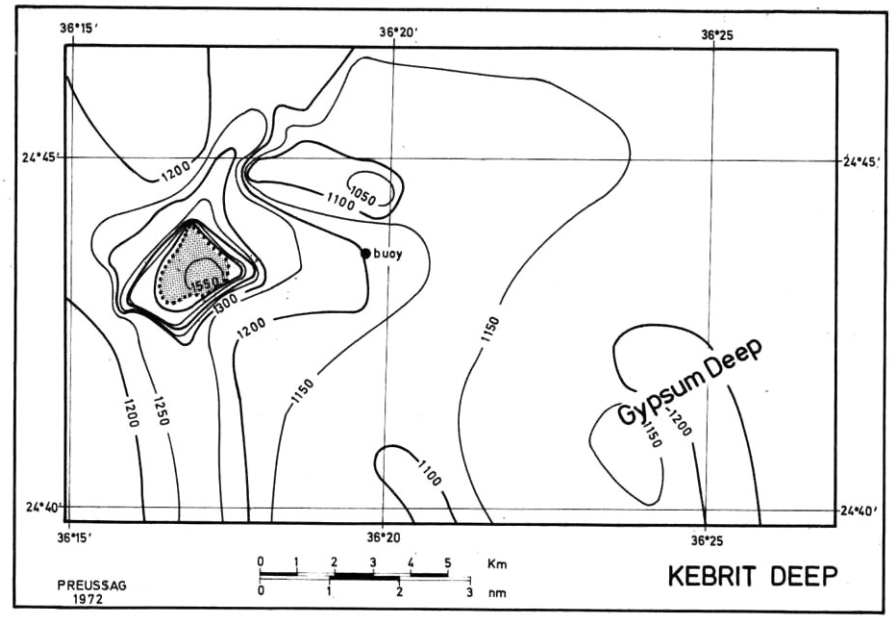

Fig. 6 Bathymetric chart of the Kebrit Deep area. ELAC narrow beam echo sounder (30 kHz, ±1.4° beam width). Contours in metre, corrected after Matthews[13]. Navigation with radar and bearing (buoy). Tracks irregular, radially from the centre of Kebrit Deep.

increased Fe and Mn content are often found in the sediments above the basalt along the central rift zone. This is consistent with observations made in the basal 40 m of Glomar Challenger cores near the Mid-Atlantic Ridge[10].

In the deeps with the strongest hydrothermal influence the bottom is covered by multicoloured sediments with extremely high sedimentation rates. Tectonic events cause repeated changes of the physico-chemical conditions and, therefore, different facies of the sediments. Normal oxidic conditions (especially during mixing with sea-water) lead to sediments with attributions of limonite, haematite and manganite facies. Sulphides are present only as pyrite and chalcopyrite.

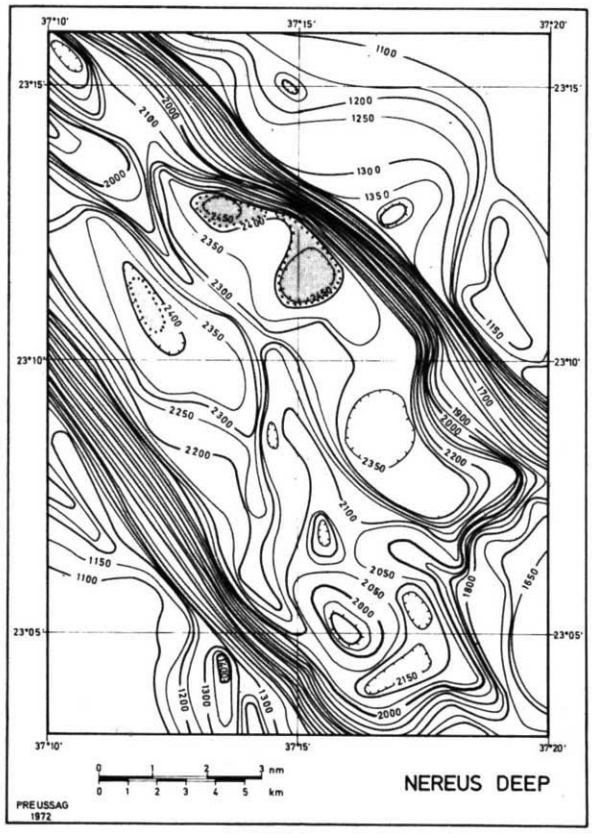

Fig. 7 Bathymetric chart of the central part of Nereus Deep. Explanation see Fig. 3. Track distance 1.8 km.

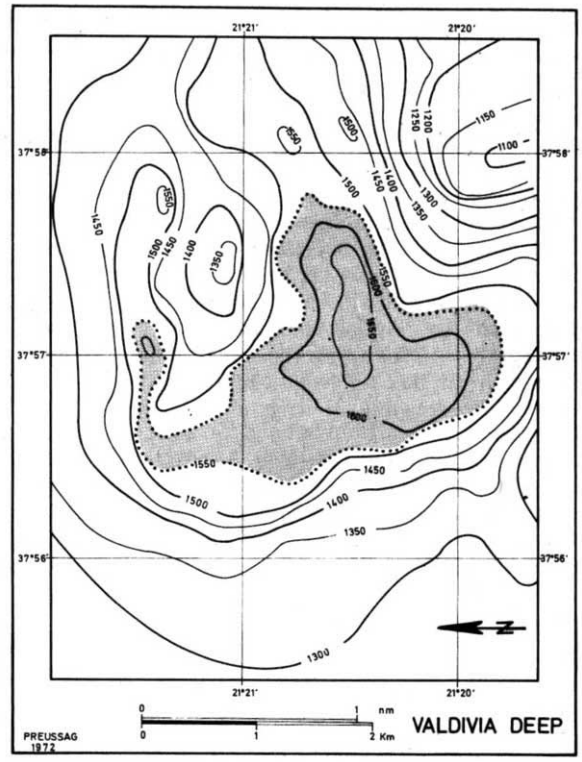

Fig. 8 Bathymetric chart of the Valdivia Deep. Explanation see Fig. 3. Track distance 500 m plus additional cross lines.

Under reduction conditions a sediment containing iron monosulphide and sphalerite together with Fe-montmorillonite and some manganosiderite is formed, but the presence of hydrogen sulphide is very important. There is also a high content of anhydrite in Atlantis II Deep and of gypsum in Gypsum Deep well crystallized, dispersed in the other facies. The sediments in Valdivia Deep, Kebrit and probably Oceanographer Deep are predominantly carbonatic. The grain size of the hydrothermal part of the sediments is extremely small, mostly below 0.002 mm. The iron content in the limonite and the haematite facies is between 50 and 65%. In the Chain Deeps manganese contents show an average of between 30 and 40%. In Atlantis II Deep some sulphide layers have a zinc content of about 20%. But continuously changing facies conditions reduced the average content of the base metals to a few per cent.

The Valdivia cruises (VA 1 and VA 3) are sponsored by the Ministry of Education and Science, Bonn, and by Preussag AG, Hannover. The bathymetric mapping was done by H. Richter and K. Lange. D. Menz supplied the chemical analyses.

Received August 21; revised September 26, 1972.

[1] Bruneau, L., Jerlov, N. G., and Koczy, F., *Rep. Swedish Deep Sea Expedition*, **3**, 99 (1953).
[2] Swallow, J. C., and Crease, J., *Nature*, **205**, 165 (1965).
[3] Miller, A. R., Densmore, C. D., Degens, E. T., Hathaway, J. C., Manheim, F. T., McFarlin, P. F., Pocklington, R., and Jokela, A., *Geochim. Cosmochim. Acta*, **30**, 341 (1966).
[4] Ross, D. A., and Hunt, I. M., *Nature*, **213**, 687 (1967).
[5] *Hot Brines and Recent Heavy Metal Deposits in the Red Sea* (edit. by Degens, E. T., and Ross, D. A.) (Springer, New York, 1969).
[6] Fairhead, J. D., and Girdler, R. W., *Phil. Trans. Roy. Soc. Lond.*, A, **267**, 47 (1970).
[7] Ben-Menahem, A., and Aboodi, E., *J. Geophys. Res.*, **76**, 2674 (1971).
[8] Girdler, R. W., *Phil. Trans. Roy. Soc. Lond.*, A, **267**, 191 (1970).
[9] Schoell, M., and Stahl, W., *Earth Planet. Sci. Lett.*, **15**, 206 (1972).
[10] Boström, K., *Nature*, **227**, 104 (1970).
[11] Schoell, M., and Hartmann, M., *Marine Geol.* (in the press).
[12] Hartmann, M., *Mar. Geol.*, **12**, M16 (1972).
[13] Matthews, D. J., *Publ. HD 282* (Hydrographic Department, Admiralty, 1939).

LETTERS TO NATURE

High Frequency Observations of the Second Radio Flare in Cygnus X-3

THE radio source identified with Cygnus X-3 was observed throughout the second great flare from 0100 UT on September 20, 1972, until 0800 UT on September 22, 1972, at 15.5 GHz using the 120-foot antenna of the Haystack Observatory in Westford, Massachusetts. In addition, two measurements were made at 22.235 GHz on September 21 and one was made at 8.105 GHz on September 22. The beginning of a third large flare is also present in our data.

From September 2 to 11 a radio flare two orders of magnitude brighter than the normal flare activity of this source was widely reported[1-3] following the initial announcement[4]. On that occasion the flux followed a rapid rise to approximately 20 f.u., before decaying in what evolved into a power law light curve.

Following notification that a second flare was in progress we started observing Cygnus X-3 at 15.5 GHz and continued to monitor its activity at regular intervals. Our objective was to observe the flare with as high a frequency as possible. The generally poor weather conditions precluded observing at 22.2 GHz except on two occasions. We were able to follow the second flare completely and observe the start of a third flare.

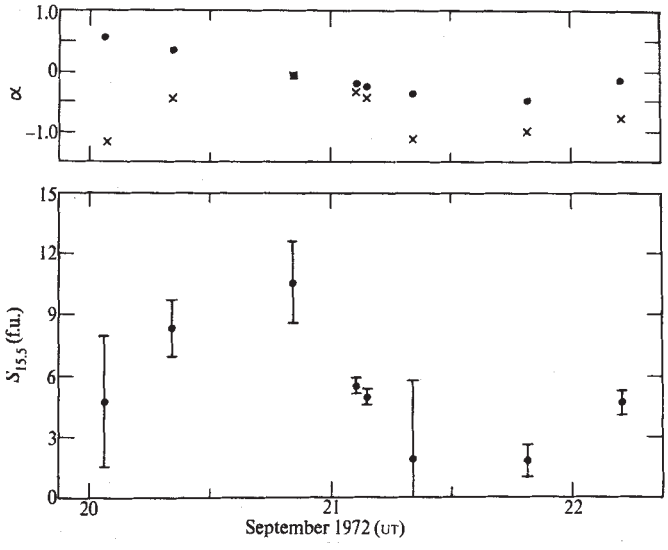

Fig. 1 The flux density of the radio source in Cygnus X-3 at 15.5 GHz as a function of UT for the period September 20–22, 1972. Above, the spectral index[7] between 2.7 GHz and 8.1 GHz (●), and the spectral index between their 8.1 GHz flux and our 15.5 GHz values (×).

The procedure of measurement consists of peaking up on the source followed by a series of on-source and off-source (±0.196° in azimuth) measurements[5]. Each measurement of the flare was preceded or followed by a calibration run on DR 21. The flux of the flare was determined relative to that of the HII region DR 21, for which we have adopted fluxes of 21.7, 20.3 and 19.2 f.u. at frequencies 8.1, 15.5 and 22.2 GHz respectively[6]. The proximity of DR 21 to the source under observation also enabled us to remove instrumental and atmospheric variations from the measurements.

Table 1 Flux of Cyg X-3 during Radio Outbursts

Day	UT	Frequencies GHz	S_ν (f.u.)	$\alpha_{8.1}^{15.5}$	Comments
September 20	0130	15.5	4.72±3.25	−1.15	
	0815	15.5	8.38±1.42	−0.44	
	2000	15.5	10.56±2.03	−0.06	
September 21	0000	22.2	4.97±0.25	—	$\alpha_{15}^{22} \simeq -0.9$
	0230	15.5	5.52±0.4	−0.30	
	0330	15.5	4.97±0.4	−0.41	
	0800	15.5	2.90±3.85	−1.1	Polarization rotating by error
	1930	15.5	1.80±0.80	−1.02	
September 22	0230	8.1	5.65±0.26	—	S_ν(8.085 GHz)= 5.4 f.u. (ref. 7)
	0500	15.5	4.71±0.6	−0.75	

The data are presented in Table 1 where S_ν is the flux density. The spectral index $\alpha_{8.1}^{15.5}$ between the 15.5 GHz measurements and the 8.085 GHz measurements of Hjellming and Balick[7] is given in column 5 and is plotted with the flux density against time in Fig. 1. The data indicate the peaking of the second flare at 15.5 GHz occurred at ~2000 UT, September 20.

From the spectral indices we can construct the spectrum of the source at three different times—before, during and after the second flux maximum (Fig. 2*a*, *b* and *c*). To explain the shapes of the spectra, we picture continual injection of relativistic electrons into a constantly expanding synchrotron emission source till the time t_2, the flare maximum. With the source electron distribution to be described by $N(E) \sim E^{-\gamma}$, at time t_1 the source had a γ of ~3 and was optically thick for the radiation below ~10 GHz. Taking 10 GHz to be the cut-off frequency where the optical depth was 1 and the size of